

Rick Ubic,* Yi Hu and Isaac
AbrahamsCentre for Materials Research, Queen Mary,
University of London, England

Correspondence e-mail: r.ubic@qmul.ac.uk

Neutron and electron diffraction studies of
 $\text{La}(\text{Zn}_{1/2}\text{Ti}_{1/2})\text{O}_3$ perovskite

Received 22 July 2005

Accepted 27 April 2006

The crystallography and microwave dielectric properties of $\text{La}(\text{Zn}_{1/2}\text{Ti}_{1/2})\text{O}_3$ (LZT) ceramics prepared *via* the mixed-oxide route were investigated in this study. While samples were largely single phase, small amounts of ZnO impurity were detected in sintered pellets. Observed reflections in electron and neutron diffraction patterns indicate that the symmetry of LZT is $P2_1/n$. The *B* site is ordered on {110} or pseudocubic {111}, but the presence of the pseudocubic $\frac{1}{2}(111)$ reflection is in itself insufficient to indicate the existence of such order. Rietveld refinements of the neutron diffraction data yield an excellent fit for such a model. The structure is highly twinned, with variants related through common {211} composition planes and 90° rotations about $\langle 011 \rangle$. The microwave dielectric properties measured were $\epsilon_r = 34$, $Qf = 36\,090$ and $\tau_f = -70 \text{ MK}^{-1}$.

1. Introduction

Microwave resonators are used extensively in telecommunications equipment, including cellular telephones and satellite links, and are at the heart of a multi-billion dollar market. Oxide ceramics are critical elements in these devices, and three properties are important in determining their usefulness as dielectric resonators. First, the material must have a high dielectric constant (ϵ_r) to enable size reduction. Second, a high quality factor, Q ($1/\tan\delta$), means fine frequency tunability and better filters. Third, these ceramics compensate for frequency drift because of their low-temperature coefficient of resonant frequency (τ_f).

Perovskite is a term used to describe an ABO_3 arrangement of cations and O anions that is isomorphous with CaTiO_3 , that is, corner-shared anion octahedra enclosing a single cation. This structure has been illustrated, for example, in the review by Ubic *et al.* (1998). The basic principles for tuning τ_f in complex perovskites have already been established. Colla *et al.* (1992, 1993) and Reaney *et al.* (1994) have shown that temperature stability in Ba- and Sr-based complex perovskites is fundamentally related to the onset and degree of octahedral tilting. Moreover, τ_f can be tuned through $\pm 300 \text{ MK}^{-1}$ without significantly altering Q or ϵ_r by manipulating the perovskite tolerance factor, t , from 1.01 to 0.93. Reducing t results in the onset of octahedral tilt transitions. The tolerance factor was first suggested by Megaw (1946) to determine the stability of the perovskite phase for a given set of ions. In general, the perovskite phase is stable when the value of t is close to unity, which is true for SrTiO_3 , for which $t = 1.00$. Reducing t results in the onset of octahedral tilt transitions and the lowering of symmetry.

The family of rare-earth zinc/magnesium titanates is of interest as possible microwave resonator materials chiefly

because of their negative τ_f values, although $\text{La}(\text{Mg}_{1/2}\text{Ti}_{1/2})\text{O}_3$ has also been considered a candidate substrate material for the growth of high- T_c superconducting films (Harshé *et al.*, 1994; Cho *et al.*, 1999), where the requirement is for low ε_r and high Q . The negative τ_f of these materials, combined with the typical ease with which perovskites accept dopants, means that solid solutions can be formulated with materials with positive values for τ_f (e.g. CaTiO_3 , SrTiO_3 *etc.*), to yield ceramics with $\tau_f \simeq 0$.

The structure of $\text{La}(\text{Mg}_{1/2}\text{Ti}_{1/2})\text{O}_3$ (LMT) was first described (Macke & Blasse, 1976; Macke, 1977) as 'probably orthorhombic' and at least partly disordered on the B site. LMT was later reported (German & Kovba, 1983) as a cubic phase with a lattice constant of $a = 7.868 \text{ \AA}$. Several years later, Negas *et al.* (1991) found LMT to be orthorhombic, but Harshé *et al.* (1994) failed to find any orthorhombic peak splitting and again suggested a cubic unit cell, but with a lattice constant of $a = 3.9195 \text{ \AA}$. LMT's average perovskite tolerance factor is 0.952, which, according to the work of Reaney *et al.* (1994), suggests the presence of both in-phase and anti-phase tilting of oxygen octahedra. Accordingly, Meden & Čeh (1998) refined the structure in the orthorhombic space group $Pbnm$, which forbids B -site ordering. More recently, LMT has been reported (Lee *et al.*, 2000; Avdeev *et al.* 2002*a,b*; Seabra, Salak *et al.*, 2003; Seabra *et al.*, 2004; Vanderah *et al.*, 2004) as an ordered perovskite in the monoclinic space group $P2_1/n$; however, LMT becomes disordered and orthorhombic when doped with very small amounts of either CaTiO_3 (Seabra, Avdeev *et al.*, 2003), SrTiO_3 (Lee *et al.*, 2000; Avdeev *et al.*, 2002*b*) or BaTiO_3 (Avdeev *et al.*, 2002*a*; Seabra *et al.*, 2004). Most recently (Vanderah *et al.*, 2004), pure $\text{La}(\text{Mg}_{1/2}\text{Ti}_{1/2})\text{O}_3$ has been ascribed lattice constants of $a = 5.5608$, $b = 5.5749$, $c = 7.8610 \text{ \AA}$, $\beta = 90.034^\circ$ in $P2_1/n$, and the structural model published by Avdeev *et al.* (2002*a*) shows the B site to be mostly ordered but with about 4% disorder.

The microwave dielectric properties of LMT have been measured by various groups. Cho *et al.* (1999) suggested that they were the first to measure such values ($\varepsilon_r = 29$, $Qf = 75\,500$ at 10 GHz and $\tau_f = -65 \text{ MK}^{-1}$), but they were in fact beaten by both a Kyocera Corporation (Kyoto, Japan) patent (Kyocera Corporation, 1987), which reported $\varepsilon_r = 32$ and $\tau_f = -88.3 \text{ MK}^{-1}$, and Negas *et al.* (1991), who published values ($\varepsilon_r = 33$, $Qf = 40\,000$ at 5 GHz and $\tau_f = -100 \text{ MK}^{-1}$) 8 years earlier. As dense samples have sometimes been difficult to prepare [*e.g.* the pellets in the work of Vanderah *et al.* (2004) were only 90% dense], there has been some variability in the measured properties. The relative permittivity varies from 27 (Salak *et al.*, 2003) to 33 (Negas *et al.*, 1991), and Qf values range from 40 000 (Negas *et al.*, 1991) to $\sim 60\,000$ (Lee *et al.*, 2000; Vanderah *et al.*, 2004) to 75 500 (Cho *et al.*, 1999) all the way up to 114 300 (Seabra, Avdeev *et al.*, 2003; Seabra, Salak *et al.*, 2003). Similarly, τ_f measurements seem to vary between groups, with values typically approximately -81 MK^{-1} (Lee *et al.*, 2000; Seabra, Avdeev *et al.*, 2003; Seabra, Salak *et al.*, 2003; Vanderah *et al.*, 2004; Kyocera Corporation, 1987; Salak *et al.*, 2003), although values of -65 MK^{-1} (Cho *et al.*, 1999) and -100 MK^{-1} (Negas *et al.*, 1991) have also been reported.

Commercially promising compositions were found by doping with either CaTiO_3 (0.44LMT–0.56CT: $\varepsilon_r = 47$, $Qf = 28\,120$ at 3.8 GHz and $\tau_f = 0$; Negas *et al.*, 1991) or BaTiO_3 (0.5LMT–0.5BT: $\varepsilon_r \simeq 60$, $Qf \simeq 9600$ and $\tau_f = -2 \text{ MK}^{-1}$; Seabra *et al.*, 2004). Kyocera Corporation (1987) holds a patent on compositions in the system $(1-x)\text{La}(\text{Mg}_{1/2}\text{Ti}_{1/2})\text{O}_3-x\text{CaTiO}_3$ ($0 \leq x \leq 0.7$), including the temperature-stable composition $x = 0.55$, for which they disclose $\varepsilon_r = 47.6$, $\tan \delta = 0.00028$ and $\tau_f = 0.6 \text{ MK}^{-1}$.

Cell constants for $\text{La}(\text{Zn}_{1/2}\text{Ti}_{1/2})\text{O}_3$ (LZT) were published by Kucheiko *et al.* (1996) (orthorhombic; $a = 5.6077$, $b = 7.8986$, $c = 5.5641 \text{ \AA}$), but no atomistic model has yet been proposed. The microwave properties they measured were $\varepsilon_r = 28.69$, $Qf = 59\,892$ and $\tau_f = -71 \text{ MK}^{-1}$, but the density of their samples was only about 90% of the theoretical density (ρ_{th}). These properties were later remeasured by Cho *et al.* (1997) on samples which were about 97% ρ_{th} . They reported $\varepsilon_r = 34$, $Qf = 59\,000$ and $\tau_f = -52 \text{ MK}^{-1}$. Like LMT, LZT is reportedly ordered but becomes disordered upon the addition of small amounts of either CaTiO_3 (Cho *et al.*, 2001) or SrTiO_3 (Cho *et al.*, 1998, 2001) dopants, although evidence of short-range order was still found by FT-IR at higher doping levels (Cho *et al.*, 2001). In the case of $x\text{SrTiO}_3-(1-x)\text{LZT}$, long-range order at the B site is lost at $x \geq 0.4$ (Cho *et al.*, 1998, 2001). A -site cation displacements and in-phase octahedral tilting are lost at $x \geq 0.6$ (Cho *et al.*, 1998), and finally antiphase tilts disappear at $x \geq 0.9$ (Cho *et al.*, 1998). As for LMT, commercially promising compositions are all doped to about the 50% level. Indeed, Yeo *et al.* (1996) reported that 0.5LZT–0.5 CaTiO_3 had $\varepsilon_r = 50$, $Qf = 38\,000$ and $\tau_f = 0$, while Cho *et al.* (1998) found that 0.5LZT–0.5 SrTiO_3 had $\varepsilon_r = 55$, $Qf \simeq 60\,000$ and $\tau_f = 0$. Kyocera Corporation (2000) have also recently developed ceramics in the system $\text{CaTiO}_3\text{--La}(\text{Zn}_{1-x}\text{M}_x)\text{O}_3$ ($M = \text{W, Ni, Co, Zr, Sn, Mn and Cu}$).

The average tolerance factor of LZT is $t = 0.947$, which, like LMT, suggests the presence of both in-phase and anti-phase tilting of oxygen octahedra. The effects of this tilting have been observed (Cho *et al.*, 2001) by X-ray diffraction (XRD) in the form of $\frac{1}{2}(311)$ and $\frac{1}{2}(310)$ superlattice reflections corresponding to anti-phase and in-phase tilting, respectively. Systematic cation displacement was also detected by the appearance of $\frac{1}{2}(210)$ reflections, and $\frac{1}{2}(111)$ reflections were observed and ascribed to the doubling of the unit cell caused by the B -site cation ordering. Based on this crystallographic evidence, three possible orthorhombic space groups can be derived for the structure ($Pmnm$, $Pnma$, $Cmcm$), none of which can also account for the B -site ordering. Single-microcrystal XRD measurements or transmission electron microscopy combined with neutron diffraction would be required to establish the structure unambiguously, and the results of such work are described here.

2. Experimental procedure

LZT samples were prepared by conventional mixed-oxide powder processing. Starting materials included La_2O_3 (99.9% Meldform Rare Earths, UK), TiO_2 (99.9% Alfa Aesar, UK)

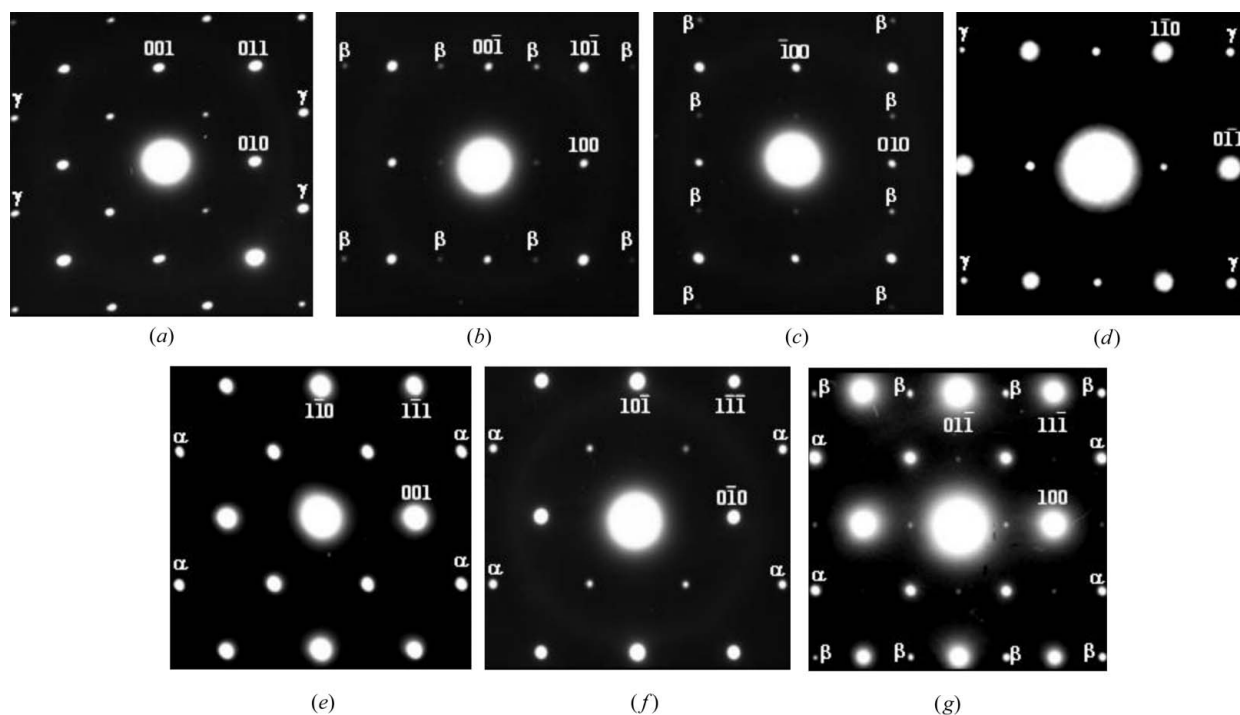


Figure 1

SADPs of LZT indexed according to the simple pseudocubic perovskite unit cell ($a = 3.9449 \text{ \AA}$) corresponding to (a) $[100]$, (b) $[010]$, (c) $[001]$, (d) $[111]$, (e) $[110]$, (f) $[101]$ and (g) $[011]$.

and ZnO (99.9% Elementis Specialties, UK). As described in detail elsewhere (Ubic *et al.*, 2005), La_2O_3 powder was first hydrated by mixing it with a surplus of distilled water and leaving it to dry overnight at 353 K. Stoichiometric amounts of all the powders were then milled together in a nylon millpot partly filled with ZrO_2 media and distilled water for 4 h. A small amount (1 wt%) of Dispex A40 (Allied Colloids, Bradford, UK) was added as a deflocculant. The slurries were then dried overnight at 353 K. Dried powders were subsequently granulated with a mortar and pestle and sieved to under $250 \mu\text{m}$. The powders were then heated to 873 K for 2 h in an open alumina crucible and allowed to cool. The powders were then mixed by hand, covered with a lid and re-heated to 1473 K for 2 h. After calcination, the powder was re-milled for a further 4 h with 2 wt% PEG 1500 (Whyte Chemicals, London) being added in aqueous solution 5–10 min before completion. These slurries were then dried at 353 K and subsequently pressed (125 MPa) into cylindrical pellets, 10 mm in diameter and 3 mm thick. These pellets were sintered in closed alumina boats for 2 h at 1773 K.

Some samples underwent thinning by ion milling (model 600, Gatan, California, USA) for observation in the transmission electron microscope (JEM 2010, Jeol, Tokyo). High-resolution neutron diffraction data were acquired on the HRPD instrument at the Rutherford Appleton Laboratory's ISIS facility (experiment number RB 14933). Data from the backscattering detector bank was analysed in the d -spacing range 0.70 – 3.94 \AA with the *General Structure Analysis System* (GSAS; Larson & Von Dreele, 1987) Rietveld refinement program. Measurements of ε_r , Q and τ_f were obtained at

Filtronic Comtek (Wolverhampton, UK) on a vector network analyser (model 8753E, Hewlett Packard, USA).¹

3. Structure of $\text{La}(\text{Zn}_{1/2}\text{Ti}_{1/2})\text{O}_3$

It is very difficult to determine the symmetry of tilted perovskites such as LZT from powder XRD alone. Peaks associated with oxygen octahedral tilting, as well as those arising from cation ordering, are very weak in XRD – hence the confusion in the early literature (Harshé *et al.*, 1994; Macke & Blasse, 1976; Macke, 1977; German & Kovba, 1983; Negas *et al.*, 1991) on the structure of LMT already described. Electron diffraction of single crystals within a ceramic has some advantages, although the interpretation of patterns can be complicated by the presence of double diffraction and twinning.

The selected-area diffraction patterns (SADPs) in Fig. 1, obtained from several grains, have been indexed self-consistently according to the simple pseudocubic perovskite unit cell ($a = 3.9449 \text{ \AA}$). Evidence of in-phase octahedral tilting can be found by examining the $\langle 100 \rangle$ pseudocubic SADPs (Figs. 1a–1c). Each pattern can reveal such tilting about a single axis by allowing, according to the Weiss zone law, a unique set of $\frac{1}{2}$ {even, odd, odd}-type γ reflections to appear. As can clearly be seen, only Fig. 1(a) contains γ reflections, indicating the presence of in-phase tilting about a single pseudocubic axis.

¹ Supplementary data for this paper are available from the IUCr electronic archives (Reference: WS5035). Services for accessing these data are described at the back of the journal.

The most efficient way of characterizing the structure for in-phase tilts is instead to examine a $\langle 111 \rangle$ pseudocubic SADP, as shown in Fig. 1(d). Such a pattern would simultaneously allow every type of γ reflection to appear and so show all in-phase tilt axes present. In agreement with Figs. 1(a)–(c), only a single γ reflection is observed in Fig. 1(d), again indicating the presence of in-phase tilting about a single axis. The presence of $\frac{1}{2}\{\text{odd, even, even}\}$ -type β reflections in Figs. 1(b) and (c) indicates a lanthanum relative displacement with components parallel to one or two pseudocubic axes. Antiphase tilting can be revealed by studying, instead, the $\langle 110 \rangle$ pseudocubic SADPs, each one allowing a single set of $\frac{1}{2}\{\text{odd, odd, odd}\}$ -type

α reflections corresponding to antiphase tilting about two possible axes. Such patterns are shown in Figs. 1(e)–(g), each of which shows the presence of superlattice α reflections. If the first of these patterns is labelled as $[110]$, then the α reflections marked correspond to $\frac{1}{2}(\text{odd, odd, odd})$, where $h \neq l$ and $k \neq l$, e.g. $\frac{1}{2}(1\bar{1}3)$. Such reflections can be evidence of antiphase tilting about either a or b ; however, as it has already been proved (Figs. 1a–d) that octahedra are rotated in-phase about a , the correct interpretation of Fig. 1(e) must be that of antiphase tilting about b . Similarly, if Fig. 1(f) is interpreted as the $[101]$ SADP then the α reflections marked correspond to $\frac{1}{2}(\text{odd, odd, odd})$, where $h \neq k$ and $k \neq l$, e.g. $\frac{1}{2}(1\bar{3}1)$. Such reflections can be evidence of antiphase tilting about either a or c ; however, again antiphase tilting about a can be discounted and the SADP interpreted as showing antiphase tilting about c . Finally, Fig. 1(g) shows the $[011]$ SADP, the α reflections of which correspond to $\frac{1}{2}(\text{odd, odd, odd})$ where $h \neq k$ and $h \neq l$, e.g. $\frac{1}{2}(3\bar{1}\bar{1})$, again demonstrating antiphase tilting about b and/or c . Thus, from the collection of superlattice reflections observed, it seems clear that LZT can be described as a perovskite with octahedra tilted in antiphase about two axes and in-phase about the third. What is left unquantified is the relative magnitude of each of these distortions.

The possible tilt systems, according to Glazer's (1972, 1975) notation, are $a^+b^-c^-$, $a^+a^-c^-$, $a^+b^-b^-$ and $a^+a^-a^-$. Howard *et al.* (2003) showed by a group theoretical approach that, in fact, the $a^+b^-c^-$, $a^+a^-c^-$ and $a^+a^-a^-$ tilt systems cannot be produced by octahedral tilting or cation ordering, leaving just $a^+b^-b^-$, corresponding to $Pmnb$ symmetry (Glazer, 1975) or $P2_1/c$ (Howard *et al.*, 2003). In either case, the basic perovskite unit is doubled in the a , b , and c directions. A new unit cell can be obtained by inscribing within the doubled pseudocubic cell a smaller one with $a = 2a_c$, $b = c = 2^{1/2}a_c$ (the subscript c indicates the undoubled pseudocubic lattice constant). In the case of LZT, $a \approx 7.8898$, $b \approx 5.5789$, $c \approx 5.5789$ Å. This orientation of the

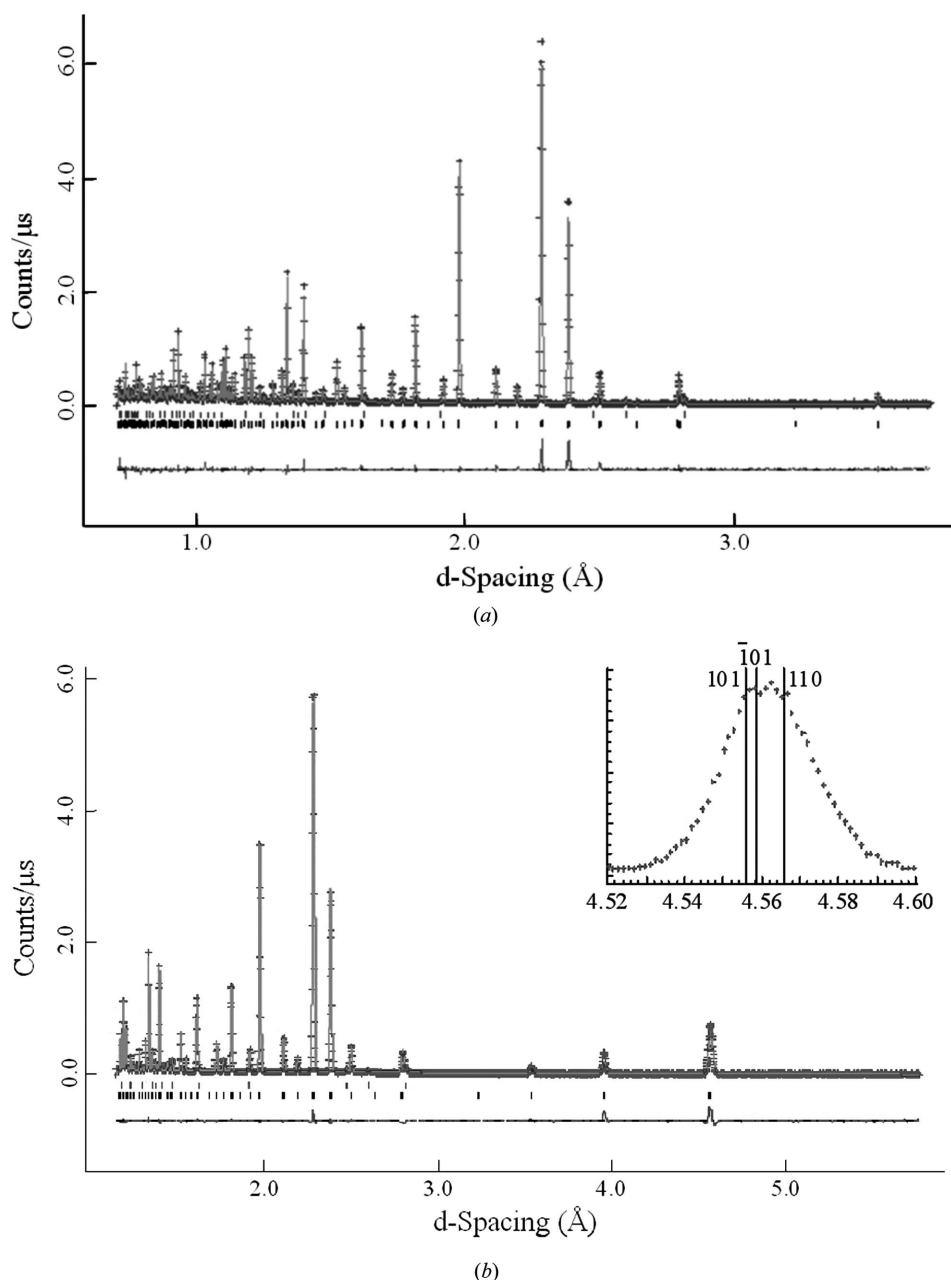


Figure 2 Neutron diffraction data from (a) the backscattered detector and (b) the 90° detector for LZT and the results of a Rietveld refinement in space group $P2_1/n$. The inset in (b) shows peak splitting indicative of a symmetry lower than tetragonal.

Table 1
Refined atomic parameters for $\text{La}(\text{Zn}_{1/2}\text{Ti}_{1/2})\text{O}_3$.

Standard uncertainties are given in parentheses.

Atom	Wyckoff	<i>x</i>	<i>y</i>	<i>z</i>	<i>U</i> _{iso}
La	4(<i>e</i>)	0.250 (2)	0.0330 (9)	0.9933 (2)	0.0168 (2)
Zn	2(<i>c</i>)	0	0.5	0	0.0232 (3)
Ti	2(<i>b</i>)	0	0	0.5	0.0160 (4)
O1	4(<i>e</i>)	0.9605 (3)	0.2059 (3)	0.2234 (3)	0.0155 (4)
O2	4(<i>e</i>)	0.9593 (3)	0.7211 (3)	0.2971 (3)	0.0200 (5)
O3	4(<i>e</i>)	0.2415 (3)	0.9837 (1)	0.4224 (2)	0.0144 (3)

unit cell corresponds to Glazer's (1972, 1975) work, although Kucenko *et al.* (1996) turned it around such that the long axis corresponded to *b*, presumably to agree with the usual description of CaTiO_3 in the standard *Pnma* setting (strangely, LMT models are typically turned such that *c* is the long axis).

The neutron diffraction pattern in Fig. 2 reveals much of the fine structure of LZT. The peak at 4.56 Å is a superlattice reflection which corresponds to $\frac{1}{2}\{111\}$ of the pseudocube or $\{101\}$ and/or $\{110\}$ of the orthorhombic/monoclinic unit cell described above. The geometrical relationship is $(101) \parallel \frac{1}{2}(111)_c$ and $(110) \parallel \frac{1}{2}(11\bar{1})_c$ (the subscript *c* again indicates indices relative to the pseudocubic axes). The appearance of such a peak in XRD is usually associated (Lee *et al.*, 2000; Avdeev *et al.*, 2002*a,b*; Seabra, Avdeev *et al.*, 2003; Seabra, Salak *et al.*, 2003; Seabra *et al.*, 2004; Cho *et al.*, 1998; Kim & Yoon, 2003; Anderson *et al.*, 1993) with cation ordering on pseudocubic $\{111\}$, although this interpretation is slightly ambiguous, as the (101) reflection is allowed in *Pmnb*, which forbids such cation order. The supposition that the existence of a peak corresponding to $\frac{1}{2}\{111\}$ always implies the existence

of cation order is generally incorrect and has no basis in the work of Glazer (1972, 1975) so often cited. For example, it is quite possible to create a disordered model of LZT in space group *Pmnb*, which shows, in calculated diffraction patterns, intensity at $d = 4.56$ Å. Such a peak corresponds to the allowed (101) reflection, equivalent to the pseudocubic $\frac{1}{2}(111)$. Such a model was developed for LMT by Meden & Čeh (1998); although not commented upon at the time, this model clearly shows intensity in this region despite the fact that Mg^{2+} and Ti^{4+} cations randomly share the *4b* positions. This finding has important implications for the study of order in complex perovskites by diffraction, the effect of order on properties, and for Raman and IR studies of order which have used diffraction experiments to calibrate the spectroscopic results.

The correct space group must instead be determined from convergent-beam electron diffraction patterns, from single-crystal XRD or by sequential Rietveld refinements. Towards this end, a first attempt at refinement was made in space group *Pmnb*. A reasonable fit ($wRp = 0.1512$, $Rp = 0.1432$, $\chi^2 = 5.349$) was obtained for this model over 556 reflections when all 14 structural variables were refined. During the process, small peaks corresponding to ZnO were noticed, and the fit improved ($wRp = 0.1395$, $Rp = 0.1358$, $\chi^2 = 4.554$) when about 2.06 wt% ZnO was included in the calculations. As *Pmnb* forbids *B*-site ordering on pseudocubic $\{111\}$, one must look to subgroups for ordered models. Examining the centrosymmetric nonisomorphic subgroups of *Pmnb*, it is readily apparent that $P2_1/n$ or $P\bar{1}$ are the only possible candidates. Space group $P\bar{1}$ would correspond to a tilt system of $a^-b^-c^-$, antiphase tilting about all three pseudocubic axes, whereas the octahedra in LZT are clearly tilted in-phase about one of these axes (Figs. 1*a* and *d*). By this process of elimination, the only symmetry left is $P2_1/n$, which implies a tilt system of $a^+b^-b^-$. Again, what is left to quantify is the relative magnitude of the antiphase tilts with respect to the in-phase tilt. Refinements of a fully ordered LZT model in $P2_1/n$ yielded the best fit of all attempted models, with $wRp = 0.0776$, $Rp = 0.0783$, $\chi^2 = 1.408$ and $R_{F2} = 0.0642$ over 1031 LZT reflections and accommodating 2.15 wt% ZnO. The lattice parameters found were $a = 7.89497$ (5), $b = 5.59640$ (3), $c = 5.58089$ (3) Å, $\beta = 90.034$ (1)°. Attempting to partially disorder the structure resulted in a reasonable fit for a narrow range of neutron times of flight (34–90 ms) corresponding to *d*-spacings of 0.70–1.86 Å. The results showed that the degree of order was about 90%, in general agreement with previous work (Macke & Blasse, 1976; Macke, 1977; Avdeev *et al.*, 2002*a*; Howard *et al.*, 2003) on similar materials; however, extending the refinement up to 190 ms ($d = 3.94$ Å) showed the degree of order to be greater than 99%. For this reason, the Rietveld refinement of neutron diffraction data shown in Fig. 2 is based on the fully ordered model in $P2_1/n$ symmetry. The fit has been extended to 5.8 Å in Fig. 2(*b*) with data from the 90° detector bank. The inset in Fig. 2(*b*) shows the broad peak at 4.56 Å split into (101) , $(\bar{1}01)$ and (110) peaks, indicating that, although $b \simeq c$ and $\beta \simeq 90^\circ$, the symmetry cannot be tetragonal.

Clearly, the unit cell is distorted only very slightly from the ideal tetragonal case ($a = 7.8898$, $b = c = 5.5789$ Å, $\beta = 90^\circ$).

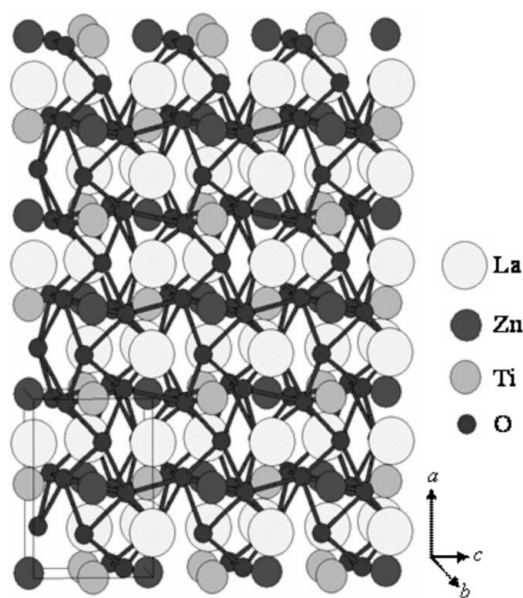


Figure 3

Diagram of the proposed crystal structure of $\text{La}(\text{Zn}_{1/2}\text{Ti}_{1/2})\text{O}_3$, viewed along a direction near $[010]$ or $[01\bar{1}]_c$.

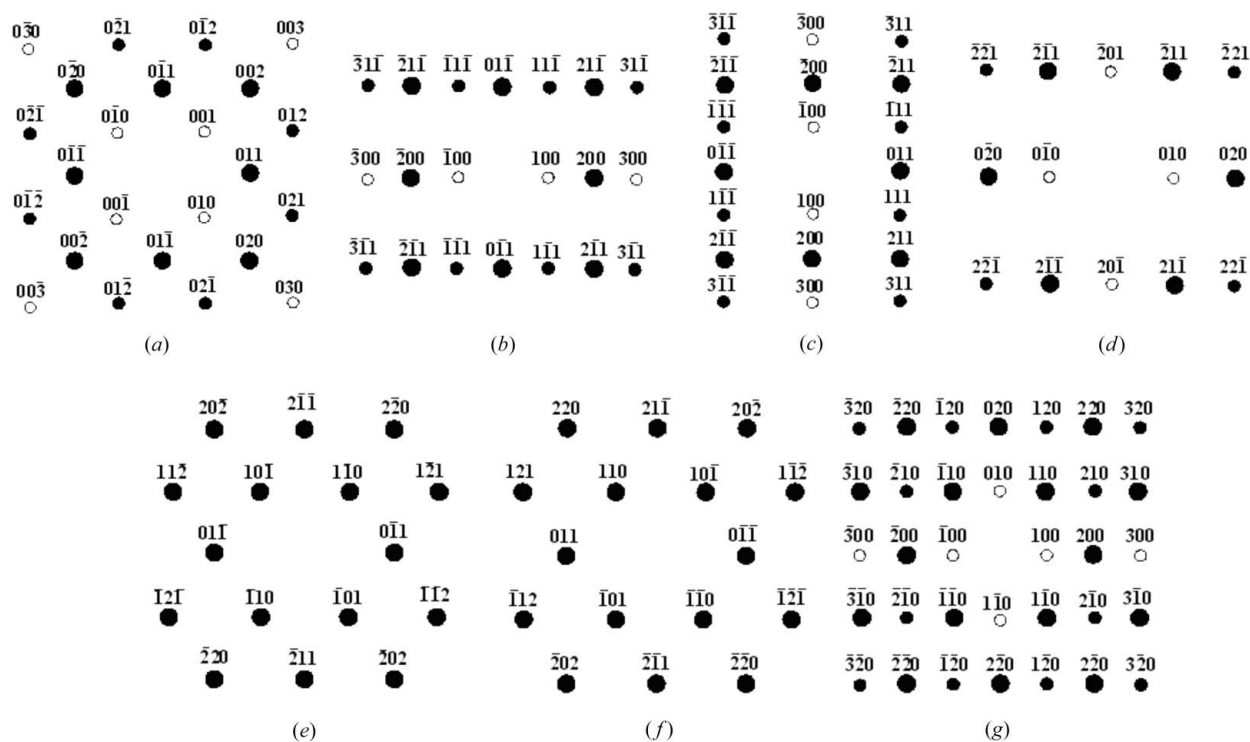


Figure 4
Schematic indexing, according to the proposed $P2_1/n$ structure, of the SADPs in Fig. 1. Solid circles represent allowed reflections, while open circles represent reflections present *via* double diffraction. (a) [100], (b) [011], (c) [011], (d) [102], (e) [111], (f) [111] and (g) [001].

Table 1 shows the calculated atomic positions, occupancies and isotropic displacement parameters for this model of LZT, and the structure is illustrated in Fig. 3. As suggested by Fig. 1, the La^{3+} positions are indeed shifted in an antiparallel fashion by 0.1050 and 0.1570 Å along [010]_c and [001]_c, respectively. The predicted in-phase tilting of octahedra about [100] is also present, with entire chains of octahedra along [100]_c tilted by ~8.3° either clockwise or anticlockwise. The antiphase tilting in the octahedral chains along [010] and [001] is a smaller effect, with octahedra in the chains tilted alternately clockwise and anticlockwise by only ~2.4°. The presence of the ZnO impurity phase is either the result of weighing errors or indicative of a nonstoichiometry in LZT, and work is currently underway to explain this impurity.

The Ti–O bond lengths range from 1.9513 to 1.9576 Å, giving an overall Ti bond-valence sum of 4.1149 (3). Similarly, the Zn–O bond lengths range from 2.0880 to 2.0938 Å, resulting in an overall bond-valence sum for Zn of 2.1135 (3). There is greater variability in the La–O bond lengths, which range from 2.4116 (La–O3) to 3.3459 Å (La–O2), yielding a La bond-valence sum of 2.92757 (8). These values are all near the ideal valencies and match well those calculated from structural models of LMT. The O–Zn–O and O–Ti–O bond angles have values of either 88.28 (7) to 91.72 (7)° and 89.56 (7) to 90.74 (7)°, respectively, and are consistent with slightly distorted octahedra.

It is important to note that the relative strength of the peak at $d = 4.56$ Å in the $P2_1/n$ space group does in fact imply some degree of cation ordering, in general agreement with work by Howard *et al.* (2003); however, such ordering cannot be

inferred by the mere presence of this peak. Indeed, this reflection does not vanish when the *B* site is randomized. Curiously, the calculated structure factors ($|F|$) for the overlapping (110) and (101) reflections decrease by 56 and 78%,

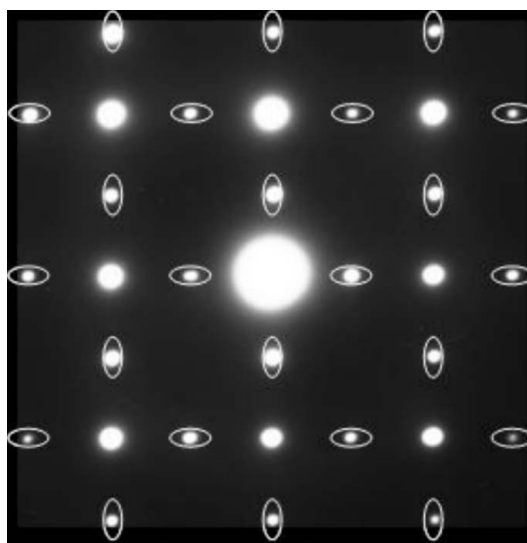


Figure 5
SADP from two overlapping twin variants related by a 90° rotation about $\langle 011 \rangle$ or pseudocubic $\langle 010 \rangle$. Horizontal ovals represent reflections from variant *A*, while vertical ovals are from variant *B*. Reflections left unmarked are common to both variants. The two variants can be indexed as [011] and [011] or [011] and [011], making the twin plane {211} type, with a $\langle 111 \rangle$ twin axis. This geometry corresponds to a pseudocubic {110} twin plane and $\langle 110 \rangle$ twin axis.

respectively, when the unit cell is disordered, but the structure factor for $(10\bar{1})$ is increased by 265%, creating an overall reduction of intensity for this peak of only 71%. Clearly, the existence of this peak cannot be used in itself to demonstrate cation order. Even for a perfectly ordered LZT structure with or without octahedral tilting, the peak would have a relative intensity in XRD of only about 1%, making it difficult to justify the adjective strong or distinguish it from a weaker version indicative of less order. Even in SADPs (Fig. 1), such spots can easily be explained in either $Pmnb$ or $P2_1/n$ by double diffraction, and some are actually allowed.

The SADPs of Fig. 1 can now be reinterpreted according to the calculated $P2_1/n$ unit cell, and the resulting indexing is shown schematically in Fig. 4.

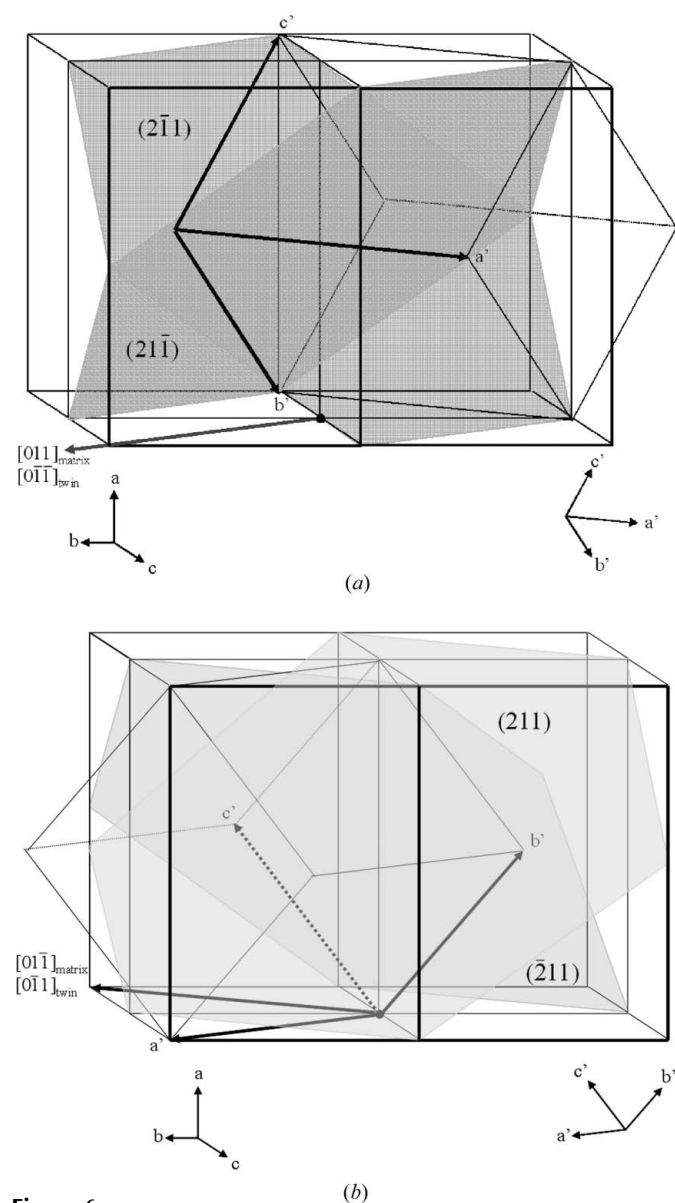


Figure 6 Diagrammatic representation of the geometrical relationship between twin variants. The twin is related to the parent by a 90° rotation about $[011]$ and a shared $(2\bar{1}1)$ or $(21\bar{1})$ twin plane in (a) or a 90° rotation about $[01\bar{1}]$ and a shared (211) or $(\bar{2}11)$ twin plane in (b).

The finding of complete order in LZT contrasts with previous work on LMT (Macke & Blasse, 1976; Macke, 1977; Avdeev *et al.*, 2002a) and its Nd analogue, $\text{Nd}(\text{Mg}_{1/2}\text{Ti}_{1/2})\text{O}_3$ (Groen *et al.*, 1986). Groen *et al.* (1986) suggest that a possible cause for the disorder may be twinning; however, LZT samples in this study also showed a high degree of twinning.

Owing to the almost exact coincidence of reflections in electron diffraction patterns, it was not possible to detect twins related by a 180° rotation about $\langle 010 \rangle_c$, which might be expected to occur; however, Fig. 5 shows evidence of twins

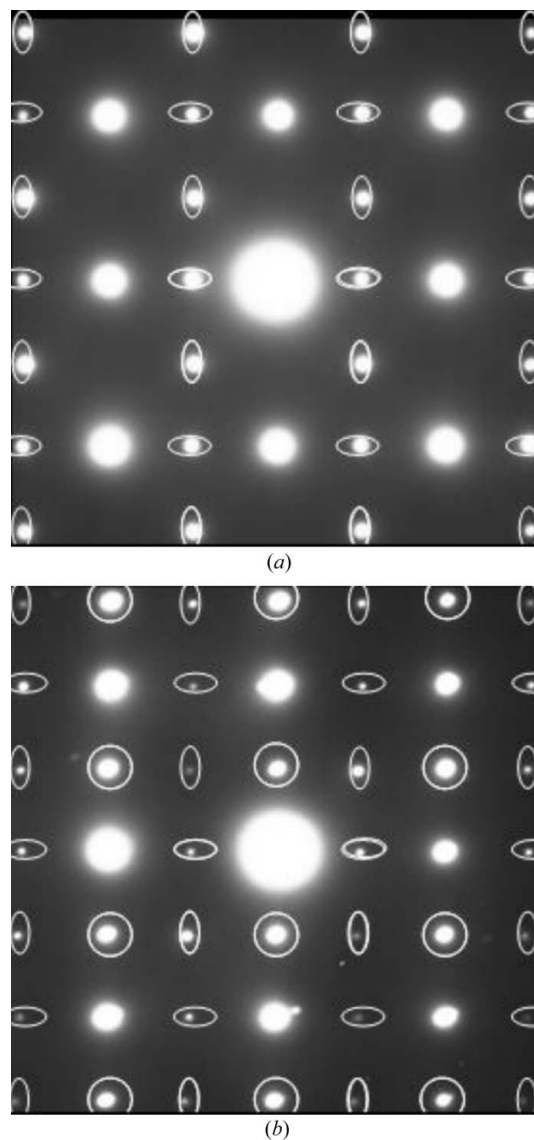


Figure 7 (a) SADP from two overlapping twin variants related by a $\{211\}$ twin plane and a 90° rotation about $\langle 011 \rangle$. Horizontal ovals represent reflections from variant A oriented along $\langle 011 \rangle$, while vertical ovals are from variant B oriented along $[100]$. Reflections left unmarked are common to both variants. (b) SADP from three overlapping twin variants related by $\{211\}$ twin planes. Horizontal ovals represent reflections from variant A oriented along $\langle 011 \rangle$; vertical ovals are from variant B oriented along $[100]$; and reflections marked with a circle arise from the third variant oriented opposite to variant A along $\langle 011 \rangle$. Reflections left unmarked are common to all three variants.

related by a 90° rotation about $\langle 011 \rangle$ or $\langle 010 \rangle_c$. A direct comparison can be made with Fig. 1(b). The variants can be indexed as $[011]$ and $[0\bar{1}\bar{1}]$, in which case the twin plane is either $(2\bar{1}\bar{1})$ or $(2\bar{1}1)$, or $[0\bar{1}\bar{1}]$ and $[01\bar{1}]$, making the twin plane either (211) or $(\bar{2}11)$. In any case, the twin axis is $\langle 111 \rangle$ or $\langle 101 \rangle_c$. Such twins have been observed previously in simple perovskites (White *et al.*, 1985). A sketch of the geometrical relationship between matrix and twin is shown in Fig. 6, with the common $(2\bar{1}\bar{1})$ and $(2\bar{1}1)$ or (211) and $(\bar{2}11)$ indicated. The twins are related to the parent LZT (four unit cells of which are shown in the figure) according to the following matrix transformations:

$$\begin{bmatrix} 0 & -1/2 & 1/2 \\ \bar{1} & -1/2 & -1/2 \\ 1 & -1/2 & -1/2 \end{bmatrix} \text{ or } \begin{bmatrix} 0 & 1/2 & 1/2 \\ 1 & -1/2 & 1/2 \\ 1 & 1/2 & -1/2 \end{bmatrix},$$

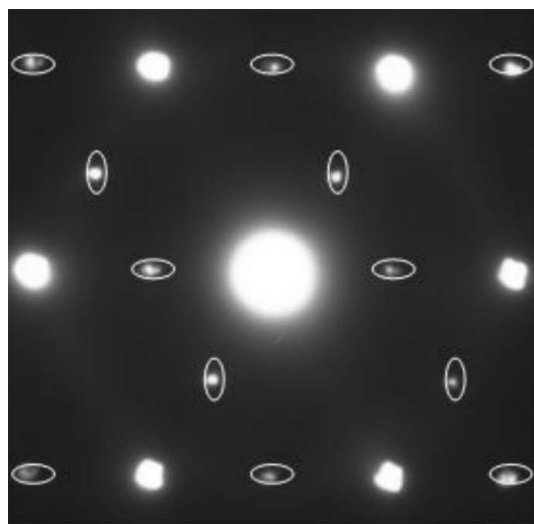
corresponding to either Fig. 5(a) (rotation about $[011]$) or 5b (rotation about $[0\bar{1}\bar{1}]$). The SADPs in Figs. 5, 7 and 8 can all be indexed with reference to Fig. 6. Fig. 7(a) can be indexed as the matrix $[011]$ SADP plus the twin-related $[100]$ SADP. The twin plane in this case is (211) , and the result is effectively an amalgam of Figs. 1(a) and 1(b). Fig. 7(b) shows the same two twin variants plus an additional one, oriented parallel to $[0\bar{1}\bar{1}]$, related to the matrix and the first twin by (211) and $(\bar{2}11)$ twin planes, respectively. Fig. 8(a) can be indexed as a combination of two twin variants oriented along $[120]$ and $[\bar{1}\bar{2}0]$, with a twin plane of $(2\bar{1}\bar{1})$, or $[\bar{1}20]$ and $[1\bar{2}0]$ with a twin plane of $(21\bar{1})$. In either case, it can easily be shown that the 60° angle between matrix and twin $\{001\}$ agrees exactly with the diagram in Fig. 6. Fig. 8(b) shows the same two variants plus a third related to the others by an additional $\{211\}$ twin plane.

The microwave properties of dense (96% ρ_{th}) LZT samples agree well in some respects with previous literature on these materials; however, disparities were noted. At 4.25 GHz, the relative permittivity was measured as $\epsilon_r = 34$. This value agrees well with most reports on LZT (Cho *et al.*, 1997, 1998, 2001); however, there is less agreement on the other properties. The best value of Qf found was 36 090 (4.25 GHz), significantly lower than the value given in most other reports. Similarly, although the measured value of τ_f , -70 MK^{-1} , agrees well with the previous work of Kucheiko *et al.* (1996), it is much lower than that reported by most other groups. As complete order was found in LZT samples in this study, it is difficult to ascribe these discrepancies, especially in Q , to the degree of order achieved. Other explanations may involve twinning or the ZnO impurity phase detected in the samples. Further investigation is warranted.

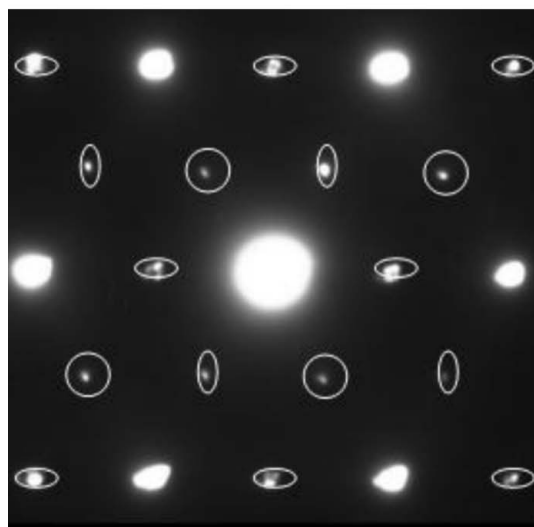
4. Conclusions

The structure of LZT has been determined by a combination of electron diffraction and Rietveld refinement of neutron diffraction data. It has monoclinic $P2_1/n$ symmetry, with lattice constants $a = 7.8950$, $b = 5.5964$, $c = 5.5809 \text{ \AA}$, $\beta = 90.034^\circ$. The B sites are completely ordered on $\{110\}$, although the presence of $\frac{1}{2}(111)$ superlattice reflections is insufficient to unambiguously establish this fact. Numerous $\{211\}$ -type twins were also observed. The microwave dielectric properties measured were $\epsilon_r = 34$, $Qf = 36\,090$ and $\tau_f = -70 \text{ MK}^{-1}$.

The authors gratefully acknowledge Dr Richard Ibberson of the Rutherford Appleton Laboratory for his help with acquiring and analysing the neutron diffraction data. In addition, raw materials were graciously supplied by Dr D. Iddles of Filtronic Comtek, Ceramics Division, Wolverhampton, UK, and electrical testing was carried out by Tim Price, also of Filtronic. Their continued contribution to this work is gratefully acknowledged.



(a)



(b)

Figure 8

(a) SADP from two overlapping twin variants related by a $\{211\}$ twin plane and a 90° rotation about $\langle 011 \rangle$. Horizontal and vertical ovals represent variants oriented oppositely along $\langle 120 \rangle$. Reflections left unmarked are common to both variants. (b) SADP from three overlapping twin variants related by $\{211\}$ twin planes. Horizontal and vertical ovals have the same meaning as in (a), and circled reflections arise from a third variant related by another $\{211\}$ twin plane and oriented similarly along $\langle 120 \rangle$. Reflections left unmarked are common to all three variants.

References

- Anderson, M. T., Greenwood, K. B., Taylor, G. A. & Poeppelmeier, K. R. (1993). *Prog. Solid State Chem.* **22**, 197–233.
- Avdeev, M., Seabra, M. P. & Ferreira, V. M. (2002a). *J. Mater. Res.* **17**, 1112–1117.
- Avdeev, M., Seabra, M. P. & Ferreira, V. M. (2002b). *Mater. Res. Bull.* **37**, 1459–1468.
- Cho, S. Y., Kim, I. T. & Hong, K. S. (1998). *Jpn. J. Appl. Phys.* **37**, 593–596.
- Cho, S. Y., Kim, C. H., Kim, D. W., Hong, K. S. & Kim, J. H. (1999). *J. Mater. Res.* **14**, 2484–2487.
- Cho, S. Y., Seo, M. K., Hong, K. S., Park, S. J. & Kim, I. T. (1997). *Mater. Res. Bull.* **32**, 725–735.
- Cho, S. Y., Youn, H. J., Lee, H. J. & Hong, K. S. (2001). *J. Am. Ceram. Soc.* **84**, 753–758.
- Colla, E. L., Reaney, I. M. & Setter, N. (1992). *Ferroelectrics*, **133**, 217–222.
- Colla, E. L., Reaney, I. M. & Setter, N. (1993). *J. Appl. Phys.* **74**, 3414–3425.
- German, M. & Kovba, L. M. (1983). *Russ. J. Inorg. Chem.* **28**, 586–587.
- Glazer, A. M. (1972). *Acta Cryst.* **B28**, 3384–3392.
- Glazer, A. M. (1975). *Acta Cryst.* **A31**, 756–762.
- Groen, W. A., Van Berkel, F. P. F. & Ijdo, D. J. W. (1986). *Acta Cryst.* **C42**, 1472–1475.
- Harshé, G., Bhalla, A. S. & Cross, L. E. (1994). *Mater. Lett.* **18**, 173–175.
- Howard, C. J., Kennedy, B. J. & Woodward, P. M. (2003). *Acta Cryst.* **B59**, 463–471.
- Kim, J. B. & Yoon, K. H. (2003). *J. Am. Ceram. Soc.* **86**, 1159–1161.
- Kucheiko, S., Kim, H. J., Yeo, D. H. & Jung, H. J. (1996). *Jpn. J. Appl. Phys.* **35**, 668–672.
- Kyocera Corporation (1987). US Patent No. 4 670 409.
- Kyocera Corporation (2000). US Patent No. 6 143 680.
- Larson, A. C. & Von Dreele, R. B. (1987). GSAS. Report No. LAUR 86–748. Los Alamos National Laboratory, New Mexico, USA.
- Lee, D. Y., Yoon, S. J., Yeo, J. H., Nahm, S., Paik, J. H., Whang, K. C. & Ahn, B. G. (2000). *J. Mater. Sci. Lett.* **19**, 131–134.
- Macke, A. J. H. (1977). *Phys. Status Solidi A: Appl. Res.* **39**, 117–123.
- Macke, A. J. H. & Blasse, G. (1976). *J. Inorg. Nucl. Chem.* **38**, 1407–1409.
- Meden, A. & Čeh, M. (1998). *Mater. Sci. Forum*, **278–281**, 773–778.
- Megaw, H. D. (1946). *Proc. Phys. Soc. London*, **58**, 133–152.
- Negas, T., Yeager, G., Bell, S. & Amren, R. (1991). *Chemistry of Electronic Ceramic Materials*, edited by P. K. Davies & R. S. Roth, pp. 21–34. Lancaster, PA, USA: Technomic Publishing Co. Inc.
- Reaney, I. M., Colla, E. L. & Setter, N. (1994). *Jpn. J. Appl. Phys.* **33**, 3984–3990.
- Salak, A. N., Seabra, M. P. & Ferreira, V. M. (2003). *J. Eur. Ceram. Soc.* **23**, 2409–2412.
- Seabra, M. P., Avdeev, M., Ferreira, V. M., Pullar, R. C. & Alford, N. McN. (2003). *J. Eur. Ceram. Soc.* **23**, 2403–2408.
- Seabra, M. P., Avdeev, M., Ferreira, V. M., Pullar, R. C., Alford, N. McN. & Reaney, I. M. (2004). *J. Am. Ceram. Soc.* **87**, 584–590.
- Seabra, M. P., Salak, A. N., Avdeev, M. & Ferreira, V. M. (2003). *J. Phys. Condens. Matter*, **15**, 4229–4238.
- Ubic, R., Khamoushi, K., Iddles, D. & Price, T. (2005). *Ceram. Trans.* **167**, 21–30.
- Ubic, R., Reaney, I. M. & Lee, W. E. (1998). *Int. Mater. Rev.* **43**, 205–219.
- Vanderah, T. A., Miller, V. L., Levin, I., Bell, S. M. & Negas, T. (2004). *J. Solid State Chem.* **177**, 2023–2038.
- White, T. J., Segall, R. L., Barry, J. C. & Hutchison, J. L. (1985). *Acta Cryst.* **B41**, 93–98.
- Yeo, D. H., Kim, J. B., Moon, J. H., Yoon, S. J. & Kim, H. J. (1996). *Jpn. J. Appl. Phys.* **35**, 663–667.